

ConvTimeNet: A Deep Hierarchical Fully Convolutional Model for Multivariate Time Series Analysis

Mingyue Cheng¹, Jiqian Yang¹, Tingyue Pan¹, Qi Liu^{1*}, Zhi Li²

¹Anhui Province Key Laboratory of Big Data Analysis and Application, University of Science and Technology of China & State Key Laboratory of Cognitive Intelligence, Hefei, China

²Shenzhen International Graduate School, Tsinghua University, Shenzhen, China
{mycheng, qiliuql}@ustc.edu.cn, {yangjq, pty12345}@mail.ustc.edu.cn, zhilizl@sz.tsinghua.edu.cn

Abstract

This paper introduces ConvTimeNet, a novel deep hierarchical fully convolutional network designed to serve as a general-purpose model for time series analysis. The key design of this network is twofold, designed to overcome the limitations of traditional convolutional networks. Firstly, we propose an adaptive segmentation of time series into sub-series level patches, treating these as fundamental modeling units. This setting avoids the sparsity semantics associated with raw point-level time steps. Secondly, we design a fully convolutional block by skillfully integrating deepwise and pointwise convolution operations, following the advanced building block style employed in Transformer encoders. This backbone network allows for the effective capture of both global sequence and cross-variable dependence, as it not only incorporates the advancements of Transformer architecture but also inherits the inherent properties of convolution. Furthermore, multi-scale representations of given time series instances can be learned by controlling the kernel size flexibly. Extensive experiments are conducted on both time series forecasting and classification tasks. The results consistently outperformed strong baselines in most situations in terms of effectiveness. The code is publicly available.¹

1 Introduction

Time series is a sequence of data points arranged in chronological order. Fully analyzing and mining this type of data [Roberts *et al.*, 2013; Kim *et al.*, 2021], such as forecasting evolving trends or classifying the target labels for a given instance, can yield significant gains in various fields, including economics, finance, and biology. Over the past decades, numerous efforts [Box *et al.*, 2015; Liu *et al.*, 2021b] have been dedicated to this area. Among these efforts, deep learning-based methods [Zhang *et al.*, 2020; Foumani *et al.*, 2023; Liu *et al.*, 2024a] have made significant progress due to their ability to model non-linear relationships and eliminate labor-intensive feature engineering.

Over a significant period in the past, the convolutional network [He *et al.*, 2016; Zheng *et al.*, 2014; Middlehurst *et al.*, 2023] has played a crucial role in time series analysis, largely due to its inherent properties that strike an excellent balance between computational efficiency and representation quality. Data back to the past years, many representative works [Bagnall *et al.*, 2017] of time series analysis typically employ convolutional networks as the backbone. For instance, temporal convolutional network (TCN[Bai *et al.*, 2018]) and its variants are widely used in modeling temporal variation dependence for the time series forecasting task. Furthermore, a large number of works (such as InceptionTime[Ismail Fawaz *et al.*, 2020], MiniRocket[Dempster *et al.*, 2021], and MCNN[Cui *et al.*, 2016]) are also proposed by employing convolutional networks to identify informative patterns from given instances in the classification of time series. However, with the advent of Transformer networks [Vaswani *et al.*, 2017; Dosovitskiy *et al.*, 2020], the role of convolutional architecture in time series analysis appears to be diminishing. Recently, Transformer-style networks [Wen *et al.*, 2022] have nearly become the dominant role in learning representations of time series, ranging from forecasting [Zhou *et al.*, 2021; Liu *et al.*, 2023] to classification tasks [Liu *et al.*, 2021a].

In reality, the primary motivation for widely employing the Transformer network is its utilization of the self-attention mechanism. This mechanism enables a more effective capture of long-term sequence dependencies. Despite their effectiveness, using Transformer networks for time series analysis also has some areas of incompatibility. Firstly, multi-scale representations, a crucial element in time series analysis, are challenging to learn within the vanilla Transformer network. This is because the self-attention mechanism can only model fixed-scale representations of sequence input. Secondly, unlike other types of sequence data, both temporal variation [Xiao *et al.*, 2022] and cross-variable dependence modeling [Fang *et al.*, 2023] are crucial for time series analysis. However, the Transformer network lacks sufficient consideration of modeling interactions across variables, which carry crucial information for accurate predictions of time series. Thirdly, it usually produces quadratic computation complexity [Zhou *et al.*, 2021] while attending very long point-wise sequence inputs. This is difficult to avoid because a numerical value at each time step can struggle to reveal informative information, resulting in very long sequence input.

*Corresponding author.

¹<https://github.com/Mingyue-Cheng/ConvTimeNet>.

Through careful analysis, we observe that these aforementioned predicaments can largely be avoided by leveraging the inherent properties of convolutional networks. Specifically, firstly, the ability to learn varying scale representations is easily achieved by maintaining a hierarchical convolutional network architecture [Cui *et al.*, 2016]. Secondly, it is established that the convolutional filter operator naturally complements the modeling of cross-variable relationships [Liu *et al.*, 2023]. When it comes to temporal dependence, the receptive field can be progressively expanded by stacking deep convolutional operations, thereby acquiring the capacity for global sequence dependence. Thirdly, convolutional neural networks are highly efficient in computation, primarily due to their weight-sharing mechanism [Han *et al.*, 2021]. This efficiency distinguishes them from Transformer networks, which are constrained by the curse of quadratic time complexity, which is directly proportional to the square of the input size. Along this line, two questions naturally arise: *what is the primary obstacle in applying current convolutional networks to time series analysis? If these barriers are overcome, can convolutional networks be revolutionized to achieve superior performance again?*

In response to the aforementioned questions, in this work, we propose a novel convolutional network, dubbed ConvTimeNet, designed to serve as a versatile model for time series analysis. One of the most distinctive features of ConvTimeNet is its use of pure convolutional operators to learn the representation of given time series data. Crucially, the network not only preserves the advanced properties of Transformer networks but also inherits several inherent strengths of convolutional networks. Specifically, we first adhere to the modern philosophy of neighboring sequence points together to avoid the sparsity semantic dilemma carried by a single numerical value. Notably, we propose to divide the raw time series into sequences of patches in a data-driven manner, which can better preserve the semantics of local regions. Secondly, on the basis of the building block in Transformer encoder networks, we design a novel fully convolutional block, where deepwise and pointwise convolutions are organized together simultaneously. Particularly, the proposed ConvTimeNet highlights that very deep and hierarchical network architectures are encouraged and very significant in modeling global receptive fields and learning multi-scale representations of given time series instances. To demonstrate the effectiveness and generic capacity of ConvTimeNet, we conduct extensive experiments over a variety of time series analysis tasks including forecasting and classification. The experimental results show that ConvTimeNet could achieve superior or competitive performance compared to strong baselines, including both advanced Transformer networks and pioneering convolutional models. We hope that the proposed ConvTimeNet can serve as an alternative and useful encoder for time series analysis.

2 A Recipe of Fully Convolutional Network for Time Series Analysis

In this section, we begin by providing a brief overview of the architecture of the newly proposed ConvTimeNet. Subsequently, we delve into two key characteristics: deformable

patch embedding and fully convolutional blocks. Finally, we demonstrate the strengths of the proposed ConvTimeNet, examining its capabilities from three distinct perspectives.

2.1 Overall Network Architecture

As illustrated in Figure 1, the forward pass of ConvTimeNet begins with the input of multivariate time series data. Before learning the representation of input data with hidden layers, we develop a deformable patch embedding layer. This layer’s primary role is to transform the raw point-wise time series input into a sequence of patch embeddings. Specifically, the selection of time series points for each patch is determined in a data-driven manner, facilitated by a predictor layer. Subsequently, the transformed time series representation is fed into a stack of full-convolution blocks, with the objective of capturing long-term dependence and learning multi-scale representations. Finally, the architecture culminates in a linear layer, designed to perform time series mining tasks such as forecasting or classification of given time series data.

2.2 Deformable Patch Embedding

The primary objective of time series analysis is to discern the correlation between data points across different time steps. In most existing studies, preserving raw point-wise time series data as input is nearly a default practice. However, a single-time step does not carry as much semantic meaning as a word in a sentence. Consequently, enhancing the information density of each input unit is crucial for improving the final results. We also note that some recent Transformer studies have begun to attempt to extract local information while analyzing their correlations. A common strategy is to aggregate neighboring time points into sub-series level patches. This process, in contrast to modeling each point-wise input individually, actually groups time points into local regions, thereby coupling their dependencies. While this approach is effective, we argue that the fixed-size patch splitting may compromise semantics, leading to reduced performance. For instance, the same pattern in different time series might have varying sizes, a concept supported by well-known shapelet-based approaches [Ye and Keogh, 2009]. Therefore, such strict patch splitting may capture inconsistent information across different instances, potentially leading to sub-optimal results.

Based on the preceding discussion, we assert that time series analysis has experienced success through patch splitting, yet substantial room for improvement remains. To address the dilemma mentioned above, we decided to adopt a philosophy of neighboring time points together, selecting specific time points within each patch in a data-driven manner. This idea of this approach is also consistent with previous work [Dai *et al.*, 2017; Chen *et al.*, 2021]. As illustrated in the lower left of Figure 1, we additionally introduced a lightweight predictor to adaptively select time points based on given vanilla features, followed by an embedding projection layer. In this study, we refer to this component as the DePatch module.

To achieve this goal, the DePatch module comprises three key steps. Formally, we denote the input time series as $X \in \mathbb{R}^{C \times T}$, where C and T indicate the number of variables (channels) and sequence lengths respectively. Before performing adaptive patch splitting, we first process the raw

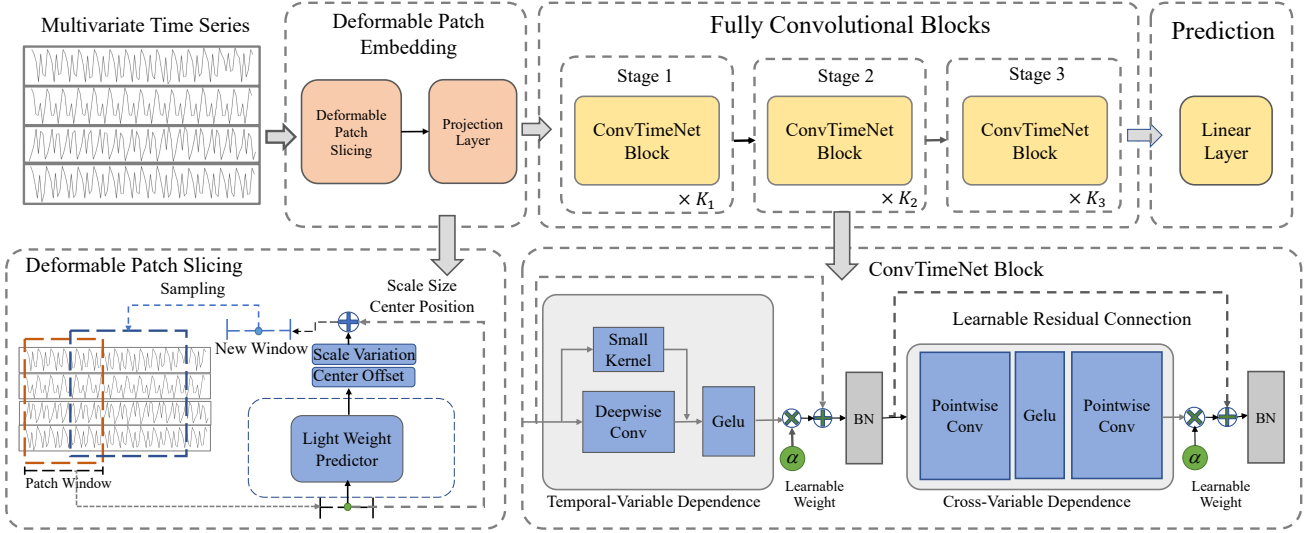


Figure 1: Illustration of the newly proposed ConvTimeNet.

time series points into $N = \lfloor \frac{T-P}{S} \rfloor + 2$ fixed-size patches, where the shape of each patch can be denoted by $x \in \mathbb{R}^{P \times C}$. We use the padding operation to ensure the uniform split. For clarity, we omit the superscript (i). Here, P denotes the corresponding patch size while S indicates the stride size of the patch window. Subsequently, each patch is assigned three key variables: the center position of this patch x_c , center offset δ_c , and scale variation δ_p . It should be noted that x_c is decided by the uniform patch splitting above while the δ_c and δ_p are obtained by borrowing the following computation process:

$$\delta_c, \delta_p = H(g(x)), \quad (1)$$

where $g(x)$ denotes the feature map obtained from input patch x , and $H(\cdot)$ indicates the lightweight predictor function. In practice, the lightweight predictor function can be instantiated by a convolutional-based projection layer. Particularly, extensive experiments over the experimental part show its sensitivity to the final results. Along this line, the final center of patch x and its scale can be computed by

$$\begin{aligned} x_c^{new} &= x_c + \delta_c, \quad P^{new} = P + 2 * \delta_p, \\ L &= x_c^{new} - \frac{P^{new}}{2}, \quad R = x_c^{new} + \frac{P^{new}}{2}, \end{aligned} \quad (2)$$

where x_c^{new} denoted as the new center position of the patch, and P^{new} represents the new length of patch. L and R are denoted as the left and right boundary positions. Finally, based on these two positions, we perform sampling on the original sequence with linear interpolation and obtain a new patch, followed by the projection layer transforms the new patch into the embedding space. With these efforts, the DePatch module allows for the adjustment of each patch's position and scale based on the input features adaptively, thereby mitigating the semantic destruction caused by hard splitting.

2.3 Fully Convolutional Blocks

To learn high-quality data representation, past methods [He *et al.*, 2016; Vaswani *et al.*, 2017] stacked repeated building blocks, a paradigm that is also very popular in the field

of data representation learning. Typically, the Transformer block, as a classical design, has been successfully applied in various fields, and these successful applications have inspired methods in the field of time series. However, the Transformer block also has some drawbacks. Firstly, the traditional Transformer block mainly process fixed-scale input, which is not flexible enough. Secondly, the Transformer block is struggling to model the cross-variable dependencies. Finally, the computational complexity of the Transformer block is quadratic related to the length of the input sequence.

Luckily, convolution can effectively address these issues. Motivated by this, we propose a fully convolutional block, as shown in the lower right module of Figure 1. Specifically, we retain the Transformer block's innovative architecture, incorporating linear and non-linear transformations. The primary distinction lies in our utilization of temporal dependency modeling, achieved through stacking 1D kernel groups, instead of the traditional multi-head attention mechanism. Practically, we employ deepwise convolution as a 1D kernel group, as it offers efficient computational efficiency. Meanwhile we substitute the Feed-Forward Network (FFN) in the Transformer block with a 1x1-sized pointwise convolution to achieve cross-variable dependency modeling. The synergistic combination of these two convolutions effectively completing the comprehensive modeling of the temporal and cross variable dependency.

To achieve a global receptive field, we increase the depth of the model. We discard the traditional residual connection and instead adopt a learnable residual [Bachlechner *et al.*, 2021], to circumvent the overfitting issue that often arises from an increased model depth. We also verify the effectiveness of the learnable residual mechanism in our experiments. Concurrently, we utilize Batch Normalization [Ioffe and Szegedy, 2015] in fully convolution block. Furthermore, we employ larger kernels to expand the receptive field. However, in practice, we found that training with large kernels presents a greater challenge. This observation is consistent with recent research finding [Ding *et al.*, 2022]. Therefore, we intro-

duce a re-parameterization mechanism to address this issue. Due to the flexibility of convolutional networks, we can easily achieve a hierarchical architecture by altering the kernel size. We divide the entire deep network architecture into multiple distinct stages, each stage is composed of K fully convolutional blocks. Drawing upon this hierarchical architecture, the time series representation across various scales can be effectively extracted. We also explored the impact of different configurations of hierarchical structures on the model’s capabilities in the experiment.

Concretely, denote $F_{\theta}^l(\cdot)$ as the larger kernel branch and $G_{\theta}^l(\cdot)$ as the small kernel branch in l -th fully convolutional block. Note that θ represents the weight of the convolution kernel, it will be updated during gradient backpropagation. The re-parameterization mechanism is defined as follows:

$$Z_{DW}^l = \text{Gelu}(F_{\theta}^l(Z^{l-1}) + G_{\theta}^l(Z^{l-1})), \quad (3)$$

where Z^{l-1} denote the output of $l-1$ convolutional block, $Z_{DW}^l \in \mathbb{R}^{D \times M}$ represents the output deepwise convolution layer in the l -th fully convolutional block. D denoted as the number of hidden dimensions and M represents the new sequence length, which is equal to the number of patches N . During the inference phase in ConvTimeNet, a sophisticated technique is employed where the weights of the small kernel are zero padded and then combined with those of the larger kernel to form a new, unified convolutional kernel. Denote α as the learnable weights for the residual connections in deepwise convolution layer, typically initialized with 0.

$$\hat{Z}_{DW}^l = Z^{l-1} + \alpha \times Z_{DW}^l, \quad (4)$$

where \hat{Z}_{DW}^l denote the output of deepwise convolution in l -th building block. To sum up, by utilizing fully convolutional blocks, we can effectively model cross-dependencies within a single block. The design of hierarchical and large kernels for ConvTimeNet facilitates the representation learning of varying scales and the creation of a global receptive field.

2.4 Analysis of the ConvTimeNet

Through these efforts, a deep and hierarchical convolutional network has been constructed, serving as a general-purpose model for time series analysis. It is noteworthy that the proposed ConvTimeNet not only retains the advanced properties of the Transformer encoder but also inherits the pioneering convolutional network. Consequently, we explore the relationship between our ConvTimeNet and traditional convolutional networks, as well as Transformer networks.

ConvTimeNet is equipped with more modern techniques compared to traditional convolutional networks. It enhances the semantic information of the input through the use of a deformable patch module and incorporates numerous great designs from the Transformer architecture. Furthermore, unlike past convolutional methods in the time series field, we consider the convolution block from operator level and utilize deepwise convolution to enhance the computational efficiency of the model.

In comparison to the Transformer method, ConvTimeNet foregoes the complex self-attention module and instead constructs a cross-variable dependency model through the collaborative role of deepwise and pointwise convolutions. Simultaneously, due to the natural advantages of convolution, a

multi-scale architecture can be directly implemented by varying the convolution kernels. The hierarchical architecture and large kernel in ConvTimeNet endow it with the capacity to possess a global receptive field.

3 Experiments

Since this work attempts to propose a generic network architecture for time series analysis, we extensively perform experiments over two categories of mainstream time series mining tasks: forecasting and classification.

3.1 Experimental Setup

Time Series Forecasting. For the task of time series forecasting, we extensively conduct experimental evaluation over 9 well-known public datasets in our experiments, including ETT (consists of 4 subsets, i.e., ETTh1, ETTh2, ETTm1, ETTm2), Electricity, Exchange, Traffic, Weather, and Illness. To demonstrate the effectiveness of our ConvTimeNet in the prediction of time series, the following advanced approaches are selected as competitive baselines, including convolutional based, such as TimesNet[Wu *et al.*, 2022], models rooted in Multilayer Perceptrons (MLPs), like N-Hits[Challu *et al.*, 2023] and DLinear[Zeng *et al.*, 2023], and those based on Transformers, including iTransformer[Liu *et al.*, 2023], Crossformer[Zhang and Yan, 2022]. Furthermore, we have scrutinized top-tier models specifically designed for specific tasks, such as PatchTST[Nie *et al.*, 2022] and TiDE[Das *et al.*, 2023] for time series forecasting.

Time Series Classification. For the task of time series classification, our experiments are carried out on a selection of 10 representative multivariate time series datasets from the renowned UEA archive, which is consistent with recent works [Liu *et al.*, 2021a; Wu *et al.*, 2022; Cheng *et al.*, 2023a]. To demonstrate the effectiveness of our ConvTimeNet in the classification of time series, we choose the following strong competitive baselines, including self-attention based methods: FormerTime [Cheng *et al.*, 2023a], TST [Zerveas *et al.*, 2021], Convolutional based: TimesNet [Wu *et al.*, 2022], MiniRocket [Dempster *et al.*, 2021], TCN [Bai *et al.*, 2018], MCDNN [Zheng *et al.*, 2014]. In addition, MLP is also employed as our baseline. We do not choose well-known classical distance-based [Middlehurst *et al.*, 2021] and shapelet-based [Ye and Keogh, 2009; He *et al.*, 2023] approaches due to the concern of expensive computation complexity.

For all experimental results, we employed equitable parameter settings. For the evaluation of time series forecasting, We utilize Mean Squared Error (MSE) and Mean Absolute Error (MAE) as the primary metrics for model evaluation. As for classification tasks, we employ Accuracy and the F1 Score as the key indicators for assessment. **Noted that all experiments were repeated three times to report the average values. Bold numbers represent the best results and the second best are underlined.** Noted that the specific descriptions are provided in the supplement material part.

3.2 Main Results Analysis

Table 1 and Table 2 present the experimental outcomes of ConvTimeNet on the tasks of time series forecasting and classification, respectively. We will subsequently delve into a

Table 1: Experimental results of time series forecasting task evaluated by MSE and MAE.

Methods		ConvTimeNet		PatchTST		iTransformer		TiDE		MSGNet		TimesNet		Crossformer		DLinear		NHits	
Metric		MSE	MAE	MSE	MAE	MSE	MAE	MSE	MAE	MSE	MAE	MSE	MAE	MSE	MAE	MSE	MAE	MSE	MAE
ETTh1	96	0.368	0.394	0.385	0.408	0.405	0.419	0.374	<u>0.395</u>	0.423	0.440	0.421	0.438	0.390	0.417	0.375	0.396	0.423	0.444
	192	0.406	0.414	0.419	0.426	0.448	0.447	<u>0.409</u>	<u>0.417</u>	0.465	0.469	0.482	0.479	0.424	0.448	0.428	0.437	0.504	0.493
	336	0.405	0.420	<u>0.429</u>	0.434	0.482	0.470	0.435	<u>0.433</u>	0.468	0.473	0.528	0.505	0.486	0.492	0.448	0.449	0.513	0.503
	720	0.442	0.457	<u>0.446</u>	0.462	0.560	0.537	<u>0.446</u>	<u>0.460</u>	0.540	0.524	0.527	0.510	0.507	0.519	0.505	0.514	0.622	0.564
ETTh2	96	0.264	0.330	<u>0.278</u>	<u>0.341</u>	0.305	0.361	0.290	0.350	0.348	0.399	0.355	0.408	0.803	0.628	0.296	0.360	0.318	0.373
	192	0.316	0.368	<u>0.343</u>	<u>0.382</u>	0.391	0.412	0.349	0.388	0.404	0.431	0.403	0.434	1.028	0.743	0.391	0.423	0.425	0.447
	336	0.315	0.378	<u>0.372</u>	<u>0.404</u>	0.418	0.433	<u>0.371</u>	0.409	0.375	0.419	0.398	0.434	1.167	0.828	0.445	0.460	0.596	0.527
	720	0.382	0.425	<u>0.395</u>	<u>0.430</u>	0.437	0.455	0.401	0.437	0.421	0.451	0.443	0.465	1.665	1.032	0.700	0.592	1.353	0.810
ETTm1	96	0.292	0.345	<u>0.298</u>	0.345	0.306	0.360	0.310	0.352	0.309	0.362	0.331	0.372	0.345	0.394	0.303	<u>0.346</u>	0.323	0.376
	192	0.329	0.368	0.339	0.374	0.345	0.382	0.345	<u>0.372</u>	0.356	0.392	0.435	0.421	0.461	0.483	<u>0.338</u>	0.368	0.365	0.401
	336	0.363	<u>0.390</u>	0.381	0.401	0.378	0.402	0.379	0.391	0.393	0.414	0.457	0.445	0.623	0.586	<u>0.373</u>	0.389	0.400	0.423
	720	0.427	<u>0.428</u>	<u>0.428</u>	0.431	0.443	0.439	0.435	0.423	0.440	0.445	0.526	0.481	0.673	0.593	<u>0.428</u>	0.423	0.463	0.463
ETTm2	96	0.167	0.257	0.174	<u>0.261</u>	0.174	0.266	0.167	0.257	0.188	0.273	0.190	0.276	0.330	0.401	<u>0.170</u>	0.264	0.212	0.290
	192	0.222	<u>0.295</u>	0.238	<u>0.307</u>	0.247	0.315	<u>0.223</u>	0.294	0.246	0.315	0.244	0.311	0.623	0.543	<u>0.233</u>	0.311	0.270	0.330
	336	0.276	0.329	0.293	0.346	0.292	<u>0.343</u>	<u>0.277</u>	0.329	0.301	0.347	0.302	0.349	0.887	0.637	0.298	0.358	0.340	0.377
	720	0.358	0.381	0.373	0.401	0.375	0.395	<u>0.371</u>	<u>0.386</u>	0.407	0.411	0.406	0.406	0.844	0.640	0.423	0.437	0.444	0.444
Electricity	96	0.132	0.226	<u>0.138</u>	0.233	0.132	<u>0.228</u>	0.160	0.262	0.169	0.279	0.177	0.281	0.150	0.258	0.141	0.238	0.147	0.250
	192	0.148	0.241	<u>0.153</u>	<u>0.247</u>	0.154	0.249	0.174	0.275	0.188	0.296	0.193	0.295	0.175	0.284	0.154	0.251	0.154	0.261
	336	0.165	0.259	<u>0.170</u>	<u>0.263</u>	0.172	0.267	0.190	0.289	0.199	0.307	0.206	0.306	0.218	0.325	0.170	0.269	0.177	0.280
	720	<u>0.205</u>	0.293	0.206	<u>0.295</u>	0.204	0.296	0.229	0.319	0.227	0.330	0.223	0.320	0.226	0.324	0.205	0.302	0.211	0.313
Exchange	96	0.086	0.204	0.094	0.216	0.099	0.225	0.107	0.233	0.167	0.303	0.166	0.305	0.283	0.393	<u>0.087</u>	<u>0.214</u>	0.126	0.256
	192	<u>0.184</u>	<u>0.303</u>	0.191	0.311	0.206	0.329	0.201	0.323	0.302	0.402	0.303	0.413	1.087	0.804	0.164	0.298	0.381	0.455
	336	<u>0.341</u>	0.421	0.343	<u>0.427</u>	0.370	0.448	0.351	0.432	0.581	0.556	0.445	0.511	1.367	0.905	0.333	0.437	0.576	0.577
	720	0.879	0.701	<u>0.888</u>	<u>0.706</u>	0.963	0.746	0.940	0.735	2.229	1.079	1.389	0.899	1.546	0.987	0.988	0.749	2.831	1.192
Traffic	96	<u>0.376</u>	0.265	0.395	0.272	0.361	0.266	0.445	0.325	0.567	0.337	0.600	0.323	0.514	0.292	0.411	0.284	0.436	0.313
	192	<u>0.392</u>	0.271	0.411	<u>0.278</u>	0.378	0.271	0.458	0.331	0.579	0.339	0.612	0.327	0.528	0.298	0.423	0.289	0.449	0.317
	336	<u>0.405</u>	<u>0.277</u>	0.424	0.284	0.390	0.274	0.471	0.336	0.604	0.350	0.628	0.344	0.538	0.303	0.437	0.297	0.475	0.330
	720	<u>0.436</u>	<u>0.294</u>	0.453	0.300	0.424	0.291	0.500	0.352	0.637	0.359	0.657	0.349	0.559	0.312	0.467	0.316	0.517	0.350
Weather	96	0.155	<u>0.205</u>	0.147	0.197	0.162	0.212	0.178	0.229	0.160	0.217	0.168	0.225	<u>0.148</u>	0.214	0.176	0.236	0.156	0.212
	192	<u>0.200</u>	<u>0.249</u>	0.191	0.240	0.205	0.251	0.221	0.264	0.208	0.255	0.218	0.268	0.201	0.270	0.217	0.275	0.203	0.260
	336	0.252	<u>0.287</u>	0.244	0.282	0.257	0.291	0.268	0.298	0.272	0.302	0.269	0.301	<u>0.248</u>	0.311	0.264	0.315	0.266	0.319
	720	<u>0.321</u>	<u>0.335</u>	0.320	0.334	0.325	0.337	0.336	0.345	0.357	0.356	0.340	0.350	0.366	0.395	0.325	0.364	0.338	0.365
Illness	24	1.469	0.800	<u>1.657</u>	<u>0.869</u>	1.930	0.883	3.988	1.444	2.453	1.044	2.130	0.981	4.312	1.418	2.313	1.059	2.575	1.146
	36	1.450	<u>0.845</u>	<u>1.467</u>	0.813	1.807	0.904	3.937	1.432	2.628	1.021	2.312	1.013	4.034	1.319	2.402	1.102	2.676	1.128
	48	1.572	0.875	<u>1.833</u>	<u>0.913</u>	1.894	0.945	4.074	1.451	2.808	1.106	2.334	1.042	4.303	1.393	2.420	1.111	2.607	1.135
	60	1.741	0.920	2.168	1.009	<u>2.033</u>	1.013	3.981	1.434	3.008	1.157	2.051	<u>0.989</u>	0.390	0.417	2.400	1.116	2.531	1.087

comprehensive analysis of the performance of both tasks in terms of effectiveness.

Time Series Forecasting. The data presented in Table 1 unequivocally shows that ConvTimeNet delivers state-of-the-art results, outperforming in over 70% of instances across nine distinct datasets for forecasting tasks. Notably, when compared to PatchTST, ConvTimeNet demonstrates a remarkable improvement in performance, achieving an over 8% increase on the ETTh2 dataset and an impressive 11% enhancement on the illness dataset. Furthermore, when considering MSGNet[Cai *et al.*, 2023], a hierarchical model of similar structure employed on the Traffic dataset with 862 channels, we observe an exceedingly high memory consumption during training. ConvTimeNet, in stark contrast, maintains an optimal equilibrium between achieving commendable experimental results and maintaining efficiency. These outcomes emphatically underscore ConvTimeNet’s robust capabilities in time series forecasting tasks. However, it is important to note that ConvTimeNet does not consistently yield the best results in every predictive scenario. This observation suggests

that there is a potential for further refinement and exploration in enhancing the performance of convolutional models.

Time Series Classification. In the realm of classification tasks, ConvTimeNet surpasses current state-of-the-art methods in over 80% of cases across ten datasets, a fact depicted in Table 2. Compared to traditional convolutional methods such as MCNN and MDCNN, ConvTimeNet exhibits a significant improvement in classification accuracy. When juxtaposed with another general purpose network, TimesNet, ConvTimeNet shows a remarkable improvement, exceeding 14% across ten datasets. Note that MiniRocket, a traditional approach, outperformed others on the EC and EP datasets. We guess that the superior performance is likely due to its varying kernel weight design, which facilitates the extraction of more refined features.

3.3 Impacts of Deformable Patch Embedding

The deformable patch embedding plays a vital role in the performance of ConvTimeNet, masterfully tokenizing time series data through its adaptive adjustment of the patch size

Table 2: Experimental results of time series classification task evaluated by Accuracy, where full results in terms of both metrics of Accuracy and F1 score is shown in the supplement materials. Noted that – indicates that the model cannot run due to the issue of being out of memory.

Datasets	ConvTimeNet	FormerTime	TimesNet	MiniRocket	TST	MLP	TCN	MCNN	MCDCNN
AWR	0.987	0.978	<u>0.980</u>	0.972	<u>0.980</u>	0.960	0.884	0.977	<u>0.980</u>
CR	0.986	0.917	<u>0.889</u>	<u>0.981</u>	<u>0.898</u>	0.935	0.868	0.917	<u>0.870</u>
CT	0.995	<u>0.992</u>	0.984	<u>0.987</u>	0.990	0.955	0.968	0.991	0.988
EC	0.338	0.312	0.287	<u>0.327</u>	-	0.309	0.299	0.293	0.298
EP	<u>0.988</u>	0.952	0.902	0.993	0.901	0.961	0.942	0.961	0.971
FM	0.680	<u>0.650</u>	0.610	0.638	0.580	0.607	0.580	0.597	0.617
JV	0.990	0.986	0.981	<u>0.987</u>	0.986	0.983	0.974	0.977	0.978
PEMS	0.830	0.173	0.728	<u>0.795</u>	0.778	0.761	0.669	<u>0.804</u>	0.792
SRS	0.596	0.572	0.542	0.564	0.541	0.546	0.507	<u>0.574</u>	0.565
DDG	0.660	0.240	0.400	0.620	0.340	0.280	0.200	0.213	<u>0.624</u>

Table 3: Experimental results w.r.t. studying the effectiveness of deformable patch embedding.

Metric	Pointwise		Uniform Patchwise		DePatch-Conv		DePatch-Conv-Conv		DePatch-MLP	
	Accuracy	F1 Score	Accuracy	F1 Score	Accuracy	F1 Score	Accuracy	F1 Score	Accuracy	F1 Score
AWR	0.961	0.961	0.979	0.978	0.981	0.981	0.987	0.987	0.979	0.978
CR	0.958	0.957	0.982	0.981	0.965	0.966	0.986	0.986	0.972	0.972
CT	0.968	0.965	0.995	0.995	0.996	0.996	0.995	0.995	0.994	0.994
EC	0.311	0.238	0.328	0.284	0.356	0.287	0.338	0.249	0.340	0.253
EP	0.986	0.985	0.978	0.978	0.990	0.991	0.988	0.988	0.983	0.983
FM	0.550	0.547	0.663	0.662	0.677	0.676	0.680	0.677	0.647	0.645
JV	0.984	0.983	0.987	0.987	0.985	0.984	0.990	0.990	0.992	0.992
PEMS	0.753	0.746	0.813	0.806	0.817	0.809	0.830	0.823	0.821	0.810
SRS	0.554	0.535	0.578	0.563	0.591	0.585	0.596	0.594	0.574	0.571
DDG	0.527	0.472	0.540	0.515	0.560	0.553	0.660	0.652	0.267	0.160

and position. To rigorously test the effectiveness of this deformable patch mechanism, we embark on a series of experiments across ten different datasets in the realm of classification tasks. These experiments are meticulously designed to compare the outcomes of having pointwise input, implementing a uniform patch, and utilizing three distinct variants of learnable predictor networks in deformable patch. The empirical results, as detailed in Table 3, reveal a significant boost in model performance attributed to the patch operation across most datasets. Particularly noteworthy is its impact on the FM dataset, which records electroencephalogram signals under different finger movements, where it catalyzed a remarkable 20% leap in performance. The prowess of the deformable patch is further highlighted in specific cases, such as the DDG dataset, recording audio information of different animals, where employing a deformable patch configured with a two-layer convolutional network led to a substantial 22% enhancement in model performance. Among the various deformable patch configurations tested, the variant with a two-layer convolutional network emerged as the most effective. In addition, three datasets achieve the best results under the single layer convolution setting, which indicates the deformable patch module can be equipped with different predictors in various scenarios.

3.4 Effectiveness of Fully Convolutional Block

To validate the effectiveness of our designed fully convolutional block, we verify the effectiveness of the block on the forecasting task, due to space limitations, we chose three datasets for the experiment. We replace the fully convolutional block with a traditional transformer encoder block and retain the learnable residual, where the building blocks of our model comprise a minimum of six layers. It is noteworthy that under the condition of setting the transform block to six layers, the model does not exhibit obvious overfitting phenomena, possibly due to the effect of the learnable residual. This allows for a direct comparison of their forecasting capabilities, as depicted in Figure 2. In a majority of cases, the convolutional block demonstrates greater performance than the transformer encoder block. This effectively validates the superiority of the fully convolutional block in time series prediction tasks. However, on the Exchange dataset, about 5000 exchange rate data, the fully convolution block just slightly surpassing transformer encoder block. This might be attributed to the smaller sample size of the Exchange dataset, thereby causing both blocks to receive insufficient training.

3.5 Impacts of Deep Hierarchical Architecture

To gain a comprehensive understanding of how varying hierarchical structures influence model performance, we conduct an extensive series of experiments. These experiments

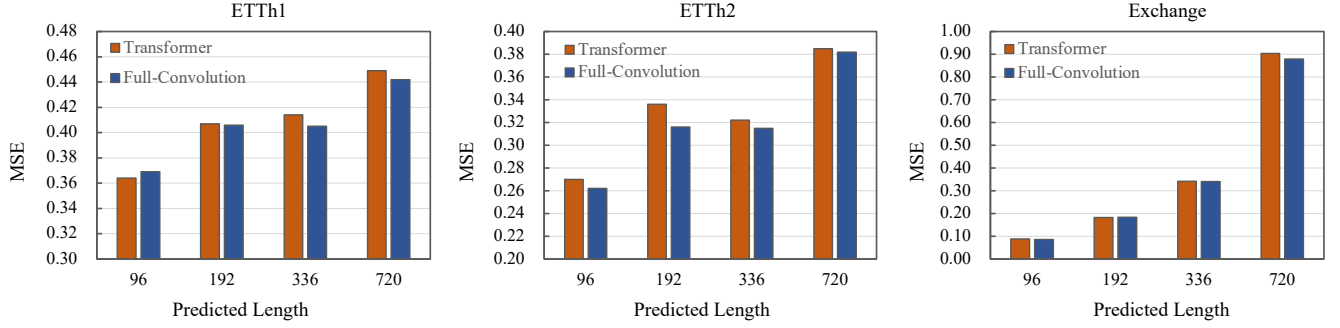


Figure 2: Performance comparison between our full-convolution block and Transformer encoder block.

Table 4: Experimental results w.r.t. studying the effectiveness of deep hierarchical architecture. This table only shows the experimental results evaluated by Accuracy while the full results can be found in the appendix part.

Models	One Stage			Two Stages			Three Stages
Setting	[7,7,7,7,7]	[13,13,13,13,13]	[19,19,19,19,19]	[7,7,7,13,13,13]	[7,7,7,19,19,19]	[13,13,13,19,19,19]	[7,7,13,13,19,19]
CT	0.992	0.994	0.995	0.995	0.993	0.995	0.995
FM	0.640	0.680	0.653	0.643	0.660	0.630	0.680
JV	0.990	0.990	0.988	0.987	0.991	0.992	0.990
Setting	[19,19,19,19,19]	[29,29,29,29,29]	[37,37,37,37,37]	[19,19,19,29,29,29]	[19,19,19,37,37,37]	[29,29,29,37,37,37]	[19,19,29,29,37,37]
CR	0.982	0.977	0.982	0.977	0.958	0.972	0.986
AWR	0.984	0.982	0.975	0.982	0.980	0.979	0.987
EC	0.347	0.345	0.342	0.338	0.340	0.337	0.338
PEMS	0.803	0.807	0.829	0.847	0.819	0.807	0.830
DDG	0.573	0.560	0.500	0.580	0.513	0.513	0.660
Setting	[37,37,37,37,37]	[43,43,43,43,43]	[53,53,53,53,53]	[37,37,37,43,43,43]	[37,37,37,53,53,53]	[43,43,43,53,53,53]	[37,37,43,43,53,53]
EP	0.988	0.983	0.981	0.980	0.978	0.976	0.988
SRS2	0.585	0.570	0.589	0.580	0.582	0.589	0.596

are conducted across ten datasets dedicated to classification tasks, utilizing seven distinct hierarchical configurations. The objective is to determine the impact of hierarchical depth and complexity on model efficacy. The results, as tabulated in Table 4, reveal a consistent trend: models configured with a three-stage hierarchical structure mostly outperform those with simpler one-stage and two-stage structures. This superior performance underscores the value of a more complex hierarchical arrangement in handling classification tasks. Notably, the experiment results demonstrate that an incremental kernel size approach to hierarchy, where each stage employ larger kernel than the previous, tends to yield more favorable outcomes in most scenarios. One plausible explanation for this observation is that as the model delves deeper and the building block kernel becomes larger, it progressively makes full use of multi-scale information.

3.6 Limitation Discussions

While our proposed ConvTimeNet generally achieves superior performance and reduced computational burden, it is essential to acknowledge its limitations in two key areas. Firstly, for certain datasets, we observed that the hierarchical hyperparameters of ConvTimeNet necessitate meticulous tuning specific to the dataset in question. This process is not only time-consuming but also adds to the implementation costs. To address this challenge, future work could explore the application of neural architecture search [Tan and Le, 2019] to facilitate the automatic tuning of hyperparameters, thereby alleviating this burden. Secondly, our study only validated the effectiveness of ConvTimeNet within the supervised learning paradigm, without extending experiments to the realm of transfer learning. Recent studies [Cheng *et al.*,

2023b] have demonstrated that self-supervised pre-training can significantly enhance the performance of deep learning architectures. Consequently, our approach might not fully realize its potential without the benefits of self-supervised pre-training. Future research could consider integrating self-supervised learning strategies with ConvTimeNet to further enhance its applicability and effectiveness.

4 Conclusion

In this study, we delved into the research question of how to reinvigorate the role of convolutional networks in time series analysis modeling. Specifically, we proposed ConvTimeNet, a deep hierarchical fully convolutional network, which can serve as a versatile backbone network for time series analysis. One key finding of ConvTimeNet is that preserving a deep and hierarchical convolutional network, equipped with modern techniques, can yield superior or competitive performance compared to the prevalent Transformer network and pioneering convolutional model. Extensive experiments conducted on the forecasting and classification of time series fully substantiate its effectiveness. Overall, we hope that ConvTimeNet can serve as an alternative model and encourage the research community to rethink the importance of convolution in time series mining tasks.

References

- [Bachlechner *et al.*, 2021] Thomas Bachlechner, Bodhisattwa Prasad Majumder, Henry Mao, Gary Cottrell, and Julian McAuley. Rezero is all you need: Fast convergence at large depth. In *Uncertainty in Artificial Intelligence*, pages 1352–1361. PMLR, 2021.
- [Bagnall *et al.*, 2017] Anthony Bagnall, Jason Lines, Aaron Bostrom, James Large, and Eamonn Keogh. The great time series classification bake off: a review and experimental evaluation of recent algorithmic advances. *Data mining and knowledge discovery*, 31:606–660, 2017.
- [Bagnall *et al.*, 2018] Anthony Bagnall, Hoang Anh Dau, Jason Lines, Michael Flynn, James Large, Aaron Bostrom, Paul Southam, and Eamonn Keogh. The uea multivariate time series classification archive, 2018. *arXiv preprint arXiv:1811.00075*, 2018.
- [Bai *et al.*, 2018] Shaojie Bai, J Zico Kolter, and Vladlen Koltun. An empirical evaluation of generic convolutional and recurrent networks for sequence modeling. *arXiv preprint arXiv:1803.01271*, 2018.
- [Box *et al.*, 2015] George EP Box, Gwilym M Jenkins, Gregory C Reinsel, and Greta M Ljung. *Time series analysis: forecasting and control*. John Wiley & Sons, 2015.
- [Cai *et al.*, 2023] Wanlin Cai, Yuxuan Liang, Xianggen Liu, Jianshuai Feng, and Yuankai Wu. Msgnet: Learning multi-scale inter-series correlations for multivariate time series forecasting. *arXiv preprint arXiv:2401.00423*, 2023.
- [Challu *et al.*, 2023] Cristian Challu, Kin G Olivares, Boris N Oreshkin, Federico Garza Ramirez, Max Mergenthaler Canseco, and Artur Dubrawski. Nhits: Neural hierarchical interpolation for time series forecasting. In *Proceedings of the AAAI Conference on Artificial Intelligence*, volume 37, pages 6989–6997, 2023.
- [Chen *et al.*, 2021] Zhiyang Chen, Yousong Zhu, Chaoyang Zhao, Guosheng Hu, Wei Zeng, Jinqiao Wang, and Ming Tang. Dpt: Deformable patch-based transformer for visual recognition. In *Proceedings of the 29th ACM International Conference on Multimedia*, pages 2899–2907, 2021.
- [Cheng *et al.*, 2023a] Mingyue Cheng, Qi Liu, Zhiding Liu, Zhi Li, Yucong Luo, and Enhong Chen. Formertime: Hierarchical multi-scale representations for multivariate time series classification. *arXiv preprint arXiv:2302.09818*, 2023.
- [Cheng *et al.*, 2023b] Mingyue Cheng, Qi Liu, Zhiding Liu, Hao Zhang, Rujiao Zhang, and Enhong Chen. Timemae: Self-supervised representations of time series with decoupled masked autoencoders. *arXiv preprint arXiv:2303.00320*, 2023.
- [Cui *et al.*, 2016] Zhicheng Cui, Wenlin Chen, and Yixin Chen. Multi-scale convolutional neural networks for time series classification. *arXiv preprint arXiv:1603.06995*, 2016.
- [Dai *et al.*, 2017] Jifeng Dai, Haozhi Qi, Yuwen Xiong, Yi Li, Guodong Zhang, Han Hu, and Yichen Wei. Deformable convolutional networks. In *Proceedings of the IEEE international conference on computer vision*, pages 764–773, 2017.
- [Das *et al.*, 2023] Abhimanyu Das, Weihao Kong, Andrew Leach, Rajat Sen, and Rose Yu. Long-term forecasting with tide: Time-series dense encoder. *arXiv preprint arXiv:2304.08424*, 2023.
- [Dempster *et al.*, 2021] Angus Dempster, Daniel F Schmidt, and Geoffrey I Webb. Minirocket: A very fast (almost) deterministic transform for time series classification. In *Proceedings of the 27th ACM SIGKDD conference on knowledge discovery & data mining*, pages 248–257, 2021.
- [Demšar, 2006] Janez Demšar. Statistical comparisons of classifiers over multiple data sets. *The Journal of Machine learning research*, 7:1–30, 2006.
- [Ding *et al.*, 2022] Xiaohan Ding, Xiangyu Zhang, Jungong Han, and Guiguang Ding. Scaling up your kernels to 31x31: Revisiting large kernel design in cnns. In *Proceedings of the IEEE/CVF conference on computer vision and pattern recognition*, pages 11963–11975, 2022.
- [Dosovitskiy *et al.*, 2020] Alexey Dosovitskiy, Lucas Beyer, Alexander Kolesnikov, Dirk Weissenborn, Xiaohua Zhai, Thomas Unterthiner, Mostafa Dehghani, Matthias Minderer, Georg Heigold, Sylvain Gelly, et al. An image is worth 16x16 words: Transformers for image recognition at scale. *arXiv preprint arXiv:2010.11929*, 2020.
- [Fang *et al.*, 2023] Yuchen Fang, Kan Ren, Caihua Shan, Yifei Shen, You Li, Weinan Zhang, Yong Yu, and Dongsheng Li. Learning decomposed spatial relations for multivariate time-series modeling. In *Proceedings of the AAAI Conference on Artificial Intelligence*, volume 37, pages 7530–7538, 2023.
- [Foumani *et al.*, 2023] Navid Mohammadi Foumani, Lynn Miller, Chang Wei Tan, Geoffrey I Webb, Germain Forestier, and Mahsa Salehi. Deep learning for time series classification and extrinsic regression: A current survey. *arXiv preprint arXiv:2302.02515*, 2023.
- [Han *et al.*, 2021] Qi Han, Zejia Fan, Qi Dai, Lei Sun, Ming-Ming Cheng, Jiaying Liu, and Jingdong Wang. On the connection between local attention and dynamic depth-wise convolution. *arXiv preprint arXiv:2106.04263*, 2021.
- [He *et al.*, 2016] Kaiming He, Xiangyu Zhang, Shaoqing Ren, and Jian Sun. Deep residual learning for image recognition. In *Proceedings of the IEEE conference on computer vision and pattern recognition*, pages 770–778, 2016.
- [He *et al.*, 2023] Wenqiang He, Mingyue Cheng, Qi Liu, and Zhi Li. Shapewordnet: An interpretable shapelet neural network for physiological signal classification. In *International Conference on Database Systems for Advanced Applications*, pages 353–369. Springer, 2023.
- [Ioffe and Szegedy, 2015] Sergey Ioffe and Christian Szegedy. Batch normalization: Accelerating deep network training by reducing internal covariate shift. In *International conference on machine learning*, pages 448–456. pmlr, 2015.
- [Ismail Fawaz *et al.*, 2020] Hassan Ismail Fawaz, Benjamin Lucas, Germain Forestier, Charlotte Pelletier, Daniel F Schmidt, Jonathan Weber, Geoffrey I Webb, Lhassane Idoumghar, Pierre-Alain Muller, and François Petitjean. Inceptiontime: Finding alexnet for time series classification. *Data Mining and Knowledge Discovery*, 34(6):1936–1962, 2020.
- [Kim *et al.*, 2021] Taesung Kim, Jinhee Kim, Yunwon Tae,

- Cheonbok Park, Jang-Ho Choi, and Jaegul Choo. Reversible instance normalization for accurate time-series forecasting against distribution shift. In *International Conference on Learning Representations*, 2021.
- [Kingma and Ba, 2014] Diederik P Kingma and Jimmy Ba. Adam: A method for stochastic optimization. *arXiv preprint arXiv:1412.6980*, 2014.
- [Liu et al., 2021a] Minghao Liu, Shengqi Ren, Siyuan Ma, Jiahui Jiao, Yizhou Chen, Zhiguang Wang, and Wei Song. Gated transformer networks for multivariate time series classification. *arXiv preprint arXiv:2103.14438*, 2021.
- [Liu et al., 2021b] Zhenyu Liu, Zhengtong Zhu, Jing Gao, and Cheng Xu. Forecast methods for time series data: a survey. *Ieee Access*, 9:91896–91912, 2021.
- [Liu et al., 2023] Yong Liu, Tengge Hu, Haoran Zhang, Haixu Wu, Shiyu Wang, Lintao Ma, and Mingsheng Long. itransformer: Inverted transformers are effective for time series forecasting. *arXiv preprint arXiv:2310.06625*, 2023.
- [Liu et al., 2024a] Zhiding Liu, Mingyue Cheng, Zhi Li, Zhenya Huang, Qi Liu, Yanhu Xie, and Enhong Chen. Adaptive normalization for non-stationary time series forecasting: A temporal slice perspective. *Advances in Neural Information Processing Systems*, 36, 2024.
- [Liu et al., 2024b] Zhiding Liu, Jiqian Yang, Mingyue Cheng, Yucong Luo, and Zhi Li. Generative pretrained hierarchical transformer for time series forecasting. *arXiv preprint arXiv:2402.16516*, 2024.
- [Middlehurst et al., 2021] Matthew Middlehurst, James Large, Michael Flynn, Jason Lines, Aaron Bostrom, and Anthony Bagnall. Hive-cote 2.0: a new meta ensemble for time series classification. *Machine Learning*, 110(11-12):3211–3243, 2021.
- [Middlehurst et al., 2023] Matthew Middlehurst, Patrick Schäfer, and Anthony Bagnall. Bake off redux: a review and experimental evaluation of recent time series classification algorithms. *arXiv preprint arXiv:2304.13029*, 2023.
- [Nie et al., 2022] Yuqi Nie, Nam H Nguyen, Phanwadee Sinthong, and Jayant Kalagnanam. A time series is worth 64 words: Long-term forecasting with transformers. *arXiv preprint arXiv:2211.14730*, 2022.
- [Paszke et al., 2019] Adam Paszke, Sam Gross, Francisco Massa, Adam Lerer, James Bradbury, Gregory Chanan, Trevor Killeen, Zeming Lin, Natalia Gimelshein, Luca Antiga, et al. Pytorch: An imperative style, high-performance deep learning library. *Advances in neural information processing systems*, 32, 2019.
- [Roberts et al., 2013] Stephen Roberts, Michael Osborne, Mark Ebdon, Steven Reece, Neale Gibson, and Suzanne Aigrain. Gaussian processes for time-series modelling. *Philosophical Transactions of the Royal Society A: Mathematical, Physical and Engineering Sciences*, 371(1984):20110550, 2013.
- [Tan and Le, 2019] Mingxing Tan and Quoc Le. Efficientnet: Rethinking model scaling for convolutional neural networks. In *International conference on machine learning*, pages 6105–6114. PMLR, 2019.
- [Vaswani et al., 2017] Ashish Vaswani, Noam Shazeer, Niki Parmar, Jakob Uszkoreit, Llion Jones, Aidan N Gomez, Łukasz Kaiser, and Illia Polosukhin. Attention is all you need. *Advances in neural information processing systems*, 30, 2017.
- [Wen et al., 2022] Qingsong Wen, Tian Zhou, Chaoli Zhang, Weiqi Chen, Ziqing Ma, Junchi Yan, and Liang Sun. Transformers in time series: A survey. *arXiv preprint arXiv:2202.07125*, 2022.
- [Wu et al., 2021] Haixu Wu, Jiehui Xu, Jianmin Wang, and Mingsheng Long. Autoformer: Decomposition transformers with auto-correlation for long-term series forecasting. *Advances in Neural Information Processing Systems*, 34:22419–22430, 2021.
- [Wu et al., 2022] Haixu Wu, Tengge Hu, Yong Liu, Hang Zhou, Jianmin Wang, and Mingsheng Long. Timesnet: Temporal 2d-variation modeling for general time series analysis. *arXiv preprint arXiv:2210.02186*, 2022.
- [Xiao et al., 2022] Qiao Xiao, Boqian Wu, Yu Zhang, Shiwei Liu, Mykola Pechenizkiy, Elena Mocanu, and Decbal Constantin Mocanu. Dynamic sparse network for time series classification: Learning what to “see”. *Advances in Neural Information Processing Systems*, 35:16849–16862, 2022.
- [Ye and Keogh, 2009] Lexiang Ye and Eamonn Keogh. Time series shapelets: a new primitive for data mining. In *Proceedings of the 15th ACM SIGKDD international conference on Knowledge discovery and data mining*, pages 947–956, 2009.
- [Zeng et al., 2023] Ailing Zeng, Muxi Chen, Lei Zhang, and Qiang Xu. Are transformers effective for time series forecasting? In *Proceedings of the AAAI conference on artificial intelligence*, volume 37, pages 11121–11128, 2023.
- [Zerveas et al., 2021] George Zerveas, Srideepika Jayaraman, Dhaval Patel, Anuradha Bhamidipaty, and Carsten Eickhoff. A transformer-based framework for multivariate time series representation learning. In *Proceedings of the 27th ACM SIGKDD conference on knowledge discovery & data mining*, pages 2114–2124, 2021.
- [Zhang and Yan, 2022] Yunhao Zhang and Junchi Yan. Crossformer: Transformer utilizing cross-dimension dependency for multivariate time series forecasting. In *The Eleventh International Conference on Learning Representations*, 2022.
- [Zhang et al., 2020] Xuchao Zhang, Yifeng Gao, Jessica Lin, and Chang-Tien Lu. Tapnet: Multivariate time series classification with attentional prototypical network. In *Proceedings of the AAAI Conference on Artificial Intelligence*, volume 34, pages 6845–6852, 2020.
- [Zheng et al., 2014] Yi Zheng, Qi Liu, Enhong Chen, Yong Ge, and J Leon Zhao. Time series classification using multi-channels deep convolutional neural networks. In *International conference on web-age information management*, pages 298–310. Springer, 2014.
- [Zhou et al., 2021] Haoyi Zhou, Shanghang Zhang, Jieqi Peng, Shuai Zhang, Jianxin Li, Hui Xiong, and Wancai Zhang. Informer: Beyond efficient transformer for long sequence time-series forecasting. In *Proceedings of the AAAI conference on artificial intelligence*, volume 35, pages 11106–11115, 2021.

A Related Work

Time series temporal and cross-variable dependency modeling are crucial aspects of time series analysis. In recent years, a variety of modeling techniques have been developed, including those rooted in Convolutional Neural Networks (CNN), Multi-Layer Perceptrons (MLP), and Transformer networks. The CNN-based methods, such as those in [Zheng *et al.*, 2014; Cui *et al.*, 2016], employ sliding convolutional kernels along the temporal dimension to capture temporal dependency. However, these methods have not yielded ideal results in modeling long-range dependencies due to the limited receptive field. On the other hand, MLP-based methods, such as those in [Zeng *et al.*, 2023; Challu *et al.*, 2023], utilize the MLP structure to encode temporal dependencies into the MLP layers. Alternatively, some methods, such as those in [Das *et al.*, 2023], can integrate covariate information into the network.

The Transformer network, renowned for its ability to capture long-range dependencies and cross-variable interactions, is particularly appealing for time series analysis. Consequently, numerous Transformer-based methods have been developed. For instance, Autoformer [Wu *et al.*, 2021] utilizes a self-correlation mechanism to capture temporal dependencies. Crossformer [Zhang and Yan, 2022] is another Transformer-based method that introduces a customized dimension segmentation embedding scheme and an explicit cross-variable attention module designed for forecasting tasks. FormerTime [Cheng *et al.*, 2023a] and GPTH [Liu *et al.*, 2024b], on the other hand, employ a hierarchical structure to capture different-scale temporal dependencies and variable dependencies. Meanwhile, the temporal patching operation [Nie *et al.*, 2022] has significantly improved the performance of the model. Despite this, the application of convolutional networks in time series analysis has gradually become less common.

As modern convolutional techniques continue to evolve, a growing number of convolutional methods are being revisited within the community. For instance, the method [Ding *et al.*, 2022] propose RepLKNet, which employs a mechanism of re-parameter to circumvent issues associated with expanding the convolutional kernel, thereby addressing the issue of receptive field limitation. Additionally, the TimesNet, introduced recently in [Wu *et al.*, 2022], considers two-dimensional temporal variations generated by periodicities, specifically designed for general tasks in time series analysis.

B Datasets

In regard to forecasting task, we adhere to the same data processing and train-validation-test set split protocol utilized in TimesNet [Wu *et al.*, 2022]. This protocol ensures the strict division of the train, validation, and test datasets based on chronological order, thereby mitigating any data leakage issues. In the time series classification task, we employ the same preprocessing approach as FormerTime [Cheng *et al.*, 2023a]. And we select ten datasets, encompassing various tasks such as gesture, action, and audio recognition, medical signal discrimination and others. Detailed information about these datasets is provided in the Table 5.

Time Series Forecasting. While for time series forecasting, we conduct experiments using nine different datasets, each of which is briefly described as follows: (1) **ETT**² encompasses records of oil temperature and load metrics of electricity transformers. The data spans from July 2016 to July 2018, divided into four sub-datasets. (2) **Electricity**³ comprises electricity usage data from 321 clients. This data covers the period from July 2016 to July 2019. (3) **Exchange**⁴ contains daily exchange rates of eight different nations. The data spans from 1990 to 2016. (4) **Traffic**⁵ provides hourly traffic volume data on San Francisco freeways, recorded by 862 sensors from 2015 to 2016. (5) **Weather**⁶ consists of 21 weather indicators, including air temperature and humidity. The data was collected at 10-minutes intervals throughout the year 2021. (6) **Illness**⁷ logs the weekly ratio of patients with influenza-like symptoms against the total patients, collected by the Centers for Disease Control and Prevention of the United States from 2002 to 2021.

In addition, we maintain a fixed length of the lookback window at 336 for ETT (ETTh1, ETTh2, ETTm1, ETTm2), Weather, Electricity, Exchange, Traffic and 104 for Illness dataset. The predicted length, varies within the range of 96, 192, 336, 720 and 24, 36, 48, 60 for Illness.

Time Series Classification. The UEA [Bagnall *et al.*, 2018] archive is recognized as one of the most comprehensive benchmarks for multivariate time series analysis. We carefully pick ten datasets that exhibit a variety of characteristics, including differing numbers and lengths of time series samples, as well as class variety. Each of the ten datasets is briefly described as follows: (1) **ArticulatoryWordRecognition** contains data collected from multiple native English speakers producing 25 words, to measure the movement of the tongue and lips. (2) **CharacterTrajectories** captures 2,858 character samples with three dimensions, to identify one of the 20 characters. (3) **Cricket** records 4 umpires motions while performing 12 cricket signals with 10 repetitions each, aiming to classify the signals based on the accelerometer data. (4) **DuckDuckGeese** is collected from recordings on www.xenocanto.com, to distinguish different bird species. (5) **Epilepsy** records data from 6 healthy participants while performing 4 different activities, and the target is to classify those activities. (6) **EthanolConcentration** records raw spectra of water-and-ethanol solutions in 44 whisky bottles, to determine the alcohol concentration. (7) **FingerMovements** records a normal subject during a no-feedback session, aiming to classify upcoming movements based on Electroencephalography (EEG) recordings from 28 channels. (8) **JapaneseVowels** records 9 Japanese-male speakers saying the vowels ‘a’ and ‘e’, to predict the speaker based on the transformed utterances. (9) **PEMS-SF** describes the occupancy rate of car lanes in the San Francisco Bay area freeways, to classify each observed day into the correct day of

²<https://github.com/zhouhaoyi/ETDataset>

³<https://archive.ics.uci.edu/ml/datasets/>

⁴<https://github.com/laiguokun/multivariate-time-series-data>

⁵<http://pems.dot.ca.gov>

⁶<https://www.bgc-jena.mpg.de/wetter/>

⁷<https://gis.cdc.gov/grasp/fluview/fluportaldashboard.html>

Table 5: The dataset descriptions are comprehensive. The variable ‘Dim’ represents the number of variables in each dataset. The term ‘Size’ refers to the total number of time steps in the (Train, Validation, Test) set. The term ‘Series Length’ in Time Series Forecasting indicates the future time steps to be predicted, and input series length in Time Series Classification. Each dataset in forecasting task comprises four prediction settings. The term ‘Frequency’ denotes the sampling interval of time steps.

Task	Dataset	Short Name	Dim	Series Length	Dataset Size	Information	Frequency
Time Series Forecasting	ETTh1, ETTh2	ETTh1, ETTh2	7	(96, 192, 336, 720)	(34465, 11521, 11521)	Electricity	15min
	ETTh1, ETTh2	ETTh1, ETTh2	7	(96, 192, 336, 720)	(8545, 2881, 2881)	Electricity	Hourly
	Electricity	Electricity	321	(96, 192, 336, 720)	(18317, 2633, 5261)	Electricity	Hourly
	Traffic	Traffic	862	(96, 192, 336, 720)	(12185, 1757, 3509)	Transportation	Hourly
	Weather	Weather	21	(96, 192, 336, 720)	(36792, 5271, 10540)	Weather	10min
	Exchange	Exchange	8	(96, 192, 336, 720)	(5120, 665, 1422)	Economy	Daily
	Illness	Ill	7	(24, 36, 48, 60)	(617, 74, 170)	Medicine	Weekly
Time Series Classification	ArticulatoryWordRecognition	AWR	9	144	(275,0,300)	Motion	200HZ
	CharacterTrajectories	CT	3	182	(1442,0,1436)	Motion	200HZ
	Cricket	CR	6	1197	(108,0,72)	HAR	184HZ
	DuckDuckGeese	DDG	1345	270	(50,0,50)	Audio	44100HZ
	Epilepsy	EP	3	206	(137,0,138)	HAR	16HZ
	EthanolConcentration	EC	3	1751	(261,0,263)	Spectro	0.5nm (of spectrum)
	FingerMovements	FM	28	50	(316,0,100)	EEG	1000HZ
	JapaneseVowels	JV	12	29	(270,0,370)	Audio	None
	PEMS-SF	PEMS	963	144	(267,0,173)	Transportation	10 minus
	SelfRegulationSCP2	SRS	7	1152	(200,0,180)	EEG	256HZ

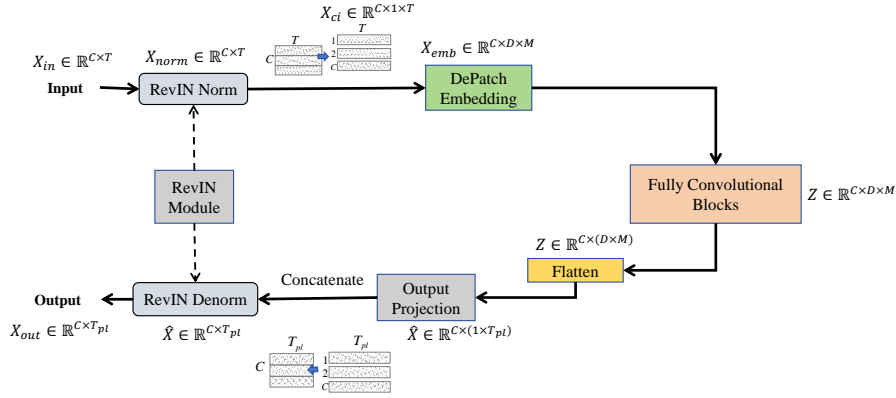


Figure 3: The pipeline of time series forecasting task.

the week. (10) **SelfRegulationSCP2** records the slow cortical potentials of an Amyotrophic Lateral Sclerosis (ALS) patient, and the task is to predict the direction of cursor movement based on the EEG data.

C Model Configuration

In both tasks, the Deformable patch slicing module employs two convolution layers as its light weight predictor. The design of the fully convolutional block remains uniform, utilizing one layer of deepwise convolution and two layers of pointwise convolution. Additionally, it incorporates learnable residual and reparameter mechanism. Generally, the small kernel size for reparameter is set to either 3 or 5.

Network for Time Series Forecasting. For time series forecasting tasks, the pipeline of forward is shown in Figure 3. The input consists of a time series with C variables, each having a specific sequence length T . We also employ the series stationarization technique from RevIN [Kim *et al.*, 2021] to mitigate the impact of distribution shifts. To ensure that the model can effectively capture multi-scale information and global receptive field, the number of fully convolution blocks is set to six or seven. For the output prediction layer, we use Flatten and Linear layers as output projection layer,

aligning with the setup of PatchTST. Denote $X_{out} \in \mathbb{R}^{C \times T_{pl}}$ as output result, where T_{pl} represents the predicted length.

Network for Time Series Classification. The pipeline of time series classification task is shown in Figure 4. The input data is a time series comprising C variables, each with a distinct sequence length T . The number of fully convolution blocks is also generally set to six. For the output layer, we employ max pooling, maintaining consistency with the FormerTime approach [Cheng *et al.*, 2023a]. The projection layer, activated with log-softmax, is designed to transform the final representation into the final probability of each class, $X_{out} \in \mathbb{R}^{C_{nc} \times 1}$, where C_{nc} represents the number of class.

D Implement Details

All experiments are conducted using PyTorch [Paszke *et al.*, 2019] on one single NVIDIA 4090 24GB GPU. The model optimization utilizes ADAM [Kingma and Ba, 2014]. For forecasting task, The number of training epochs is fixed at 10. And we use early stopping to prevent model overfitting and set patience into 3. All other hyperparameters and initialization strategies are either derived from the authors of the original works. If no open parameter script is provided, we will set up the experimental parameters according to the default

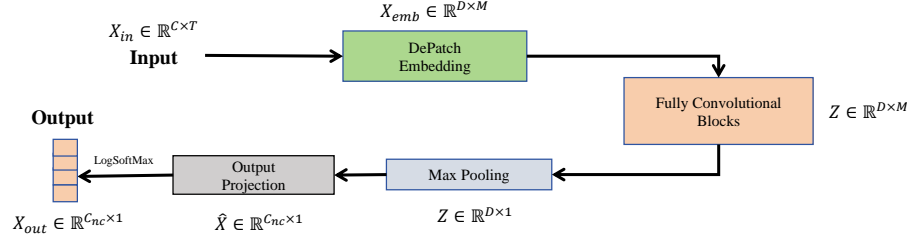


Figure 4: The pipeline of time series classification task.

Table 6: The key parameters of the experiment, where ‘DW-Kernel Size’ represents the size of the deepwise convolutional kernel in different fully convolutional blocks. ‘Patch Size’ represents the size of the patch window, and ‘Stride’ represents the stride of the patch window.

Task	Dataset	DW-Kernel Size	Patch Size	Stride	Hidden Size	Learning Rate	Dropout
Classification	ArticularyWordRecognition	19,19,29,29,37,37	32	$0.5 \times \text{Patch Size}$	64	0.001	0.1
	CharacterTrajectories	7,7,13,13,19,19	32				
	Cricket	19,19,29,29,37,37	8				
	DuckDuckGeese	19,19,29,29,37,37	8				
	Epilepsy	37,37,43,43,53,53	4				
	EthanolConcentration	19,19,29,29,37,37	32				
	FingerMovements	7,7,13,13,19,19	64				
	JapaneseVowels	7,7,13,13,19,19	4				
	PEMS-SF	19,19,29,29,37,37	16				
Forecasting	SelfRegulationSCP2	37,37,43,43,53,53	32	$0.5 \times \text{Patch Size}$	64	[0.0001,0.005]	[0.1,0.5]
	ETTh1	9,11,15,21,29,39	32				
	ETTh2	5,7,9,11,13,15	32				
	ETTm1	9,11,15,21,29,39	32				
	ETTm2	11,15,19,25,33,43,55	32				
	Traffic	15,17,21,27,35,55	32				
	Weather	9,11,15,19,25,33,43	32				
	Electricity	11,15,21,29,39,51	32				
	Exchange Rate	9,11,15,21,29,39	32				
	Illness	9,11,15,21,29,39	32				

parameter settings, with a learning rate of 0.0001, batch size of 32, and dropout of 0.2. For classification task, the model optimization utilizes ADAM as well. The number of training epochs is fixed at 200. All the baselines reproduced in this study are implemented based on the configurations outlined in the original paper or the official code.

Hyper-parameter. To ensure the reproducibility of the experiment, we have listed the hyperparameter settings for two tasks in the Table 6. The main parameters include the number of fully convolutional blocks, the varying kernel size within different blocks, the setting of the hidden size, and the range of adjustment for dropout and learning rate. In addition, we have provided experimental scripts in the open-source code, allowing users to run it directly.

In the classification task, we adopted a three-stages hierarchical structure. Each stage contains two fully convolutional blocks with equal kernel sizes. We use a six-stages or seven-stages hierarchy in forecasting tasks, with each stage containing one fully convolutional block. The trend of kernel changes in the both task is clearly from small to large. Meanwhile, we use different sizes of patch windows for different data sets, and uniformly set the sliding step of the window to half of the size of the patch, ensuring that there is an overlap of half of a continuous patch block. We also verify the effectiveness of this patch setting through experiments.

Table 7: Experimental results w.r.t. studying the effectiveness of learnable residual.

Metric	W/ Learnable Residual		W/O Learnable Residual	
	Accuracy	F1 Score	Accuracy	F1 Score
AWR	0.987	0.987	0.986	0.986
CR	0.986	0.986	0.949	0.948
CT	0.995	0.995	0.995	0.995
EC	0.338	0.249	0.331	0.266
EP	0.988	0.988	0.978	0.979
FM	0.680	0.677	0.627	0.626
JV	0.990	0.990	0.989	0.990
PEMS	0.830	0.823	0.873	0.870
SRS	0.596	0.594	0.624	0.621
DDG	0.660	0.652	0.467	0.415

E More Experimental Results

E.1 The Ablation of Learnable Residual

To mitigate the risk of overfitting potentially associated with the extensive stacking of fully convolutional blocks, we introduced the concept of learnable residual within the architecture of ConvTimeNet. This feature is specifically utilized to balance the model’s complexity with its learning capacity. To empirically evaluate the impact of learnable residual, we con-

Table 8: Experimental results w.r.t. studying the hyperparameter sensitivity of the number of fully convolutional blocks.

Depth	3 Layers		6 Layers		9 Layers	
Metric	Accuracy	F1 Score	Accuracy	F1 Score	Accuracy	F1 Score
AWR	0.978	0.978	0.987	0.987	0.988	0.988
CR	0.977	0.977	0.986	0.986	0.968	0.967
CT	0.992	0.992	0.995	0.995	0.994	0.994
EC	0.331	0.285	0.338	0.249	0.345	0.282
EP	0.978	0.978	0.988	0.988	0.986	0.986
FM	0.673	0.671	0.680	0.677	0.647	0.647
JV	0.994	0.994	0.990	0.990	0.991	0.991
PEMS	0.825	0.817	0.830	0.823	0.804	0.794
SRS	0.576	0.567	0.596	0.594	0.563	0.562
DDG	0.560	0.523	0.660	0.652	0.630	0.623

duct a series of ablation studies across ten distinct datasets, focusing on classification tasks.

The results of these studies are illuminating in Table 7. On average, the incorporation of learnable residual into ConvTimeNet led to a 4% enhancement in model performance. This improvement can likely be attributed to the learnable residual, which can dynamically adjust the contribution of each layer to the final output, enabling the model to effectively capture and represent more complex patterns in the data without succumbing to overfitting.

E.2 Performance Comparison of Varying Layer Depth

To validate the impact of the number of building blocks, we conducted experiments on ten datasets for classification tasks, varying the number of fully convolutional blocks. The results show in Table 8 indicate that stacking building blocks mostly enhances model performance. However, in most datasets, clear overfitting occurs when the number of blocks reaches nine. This could be attributed to the relatively smaller data volumes in classification tasks, which may hinder the model’s ability to undergo sufficient training.

E.3 Impact of Patch Size

The patch slicing operation is a crucial aspect of ConvTimeNet, as it determines the richness of semantic information in time series data. Therefore, we conduct experiments to assess the sensitivity of patch size on three datasets for forecasting tasks. The experimental results are presented in the Table 9, where P denotes the patch size, and S represents the stride of the patch window. The findings indicate that a bigger patch length of 32 typically achieves superior performance in most cases. Additionally, setting the stride to half of the slice length can also enhance model performance. This improvement might be attributed to the general overlap between patches, which ensures the continuity of time series semantics. Furthermore, capturing more patches within a certain length of time series data ensures a richer semantic understanding.

E.4 The Ablation of Re-parameter Mechanism

Within the fully convolutional block of our model, a re-parameter mechanism is integrated, which not only aids in gathering detailed feature insights with small kernel size but

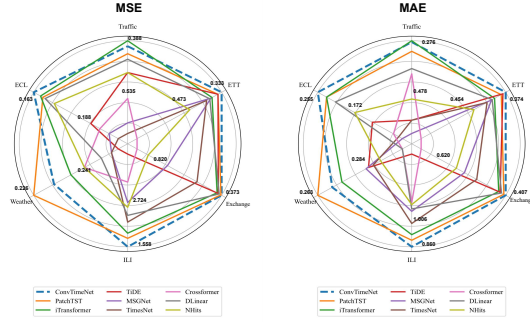


Figure 5: Model performance comparison in time series forecasting task.

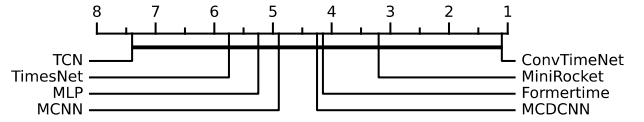


Figure 6: Critical difference diagram over the mean ranks of ConvTimeNet, baseline methods of classification task.

also greatly enable the model to expand the kernel size to be larger. To empirically evaluate the efficacy of this re-parameter mechanism, a series of ablation studies are undertaken across a variety of classification task datasets. As the result show in Table 10. Implementing the re-parameter mechanism resulted in an approximate 6% enhancement in the model’s accuracy for classification tasks. The experimental results thus strongly underscore the pivotal role that the re-parameter mechanism plays in elevating the overall performance of the model. Additionally, it is observed from the data that simply increasing the kernel size does not necessarily enhance the model’s performance in scenarios where the re-parameter mechanism is not utilized.

F Case Study Analysis

Forecasting Case. We present visual case for time series forecasting in Figure 7. These visual representations provide a clear comparison among various models. The study randomly selects a sample from the test dataset as input and plots the predicted results in all models. It can be intuitively observed from the chart that the predicted trend of ConvTimeNet is more stable compared to DLinear[Zeng *et al.*, 2023] and NHits[Challu *et al.*, 2023]. Although MSGNet[Cai *et al.*, 2023] also shows relative stability, the predicted trend of ConvTimeNet is more in line with ground truth.

Classification Case. As shown in Figure 8, we present the visual case of depatch operation. We randomly selecte two series as input to demonstrate the results of both uniform patch and deformable patch. As can be seen from the figure, the deformable patch more prominently envelops the series peaks completely. This might be attributed to the fact that the deformable patch is more sensitive to series with prominent semantic features.

Table 9: Experimental results w.r.t. studying the hyperparameter sensitivity of patch size. P denotes the patch size, and S represents the stride of the patch window.

Window Size		P=32,S=16		P=32,S=32		P=16,S=8		P=16,S=16		P=8,S=4		P=8,S=8	
Metric		MSE	MAE	MSE	MAE	MSE	MAE	MSE	MAE	MSE	MAE	MSE	MAE
ETTh1	96	0.369	0.395	0.375	0.400	0.368	0.393	0.369	0.395	0.369	0.394	0.368	0.393
	192	0.406	0.414	0.411	0.418	0.406	0.413	0.406	0.414	0.407	0.414	0.406	0.413
	336	0.405	0.420	0.407	0.425	0.405	0.420	0.405	0.422	0.410	0.425	0.405	0.421
	720	0.442	0.457	0.441	0.458	0.446	0.459	0.443	0.457	0.450	0.462	0.445	0.458
ETTm1	96	0.292	0.345	0.292	0.345	0.297	0.349	0.297	0.349	0.301	0.352	0.296	0.349
	192	0.329	0.368	0.330	0.369	0.336	0.375	0.336	0.375	0.343	0.380	0.333	0.372
	336	0.363	0.390	0.365	0.393	0.372	0.398	0.372	0.398	0.376	0.403	0.370	0.399
	720	0.427	0.428	0.427	0.427	0.435	0.434	0.435	0.434	0.440	0.437	0.433	0.432
Exchange	96	0.086	0.204	0.086	0.204	0.088	0.207	0.088	0.207	0.088	0.208	0.088	0.207
	192	0.184	0.303	0.181	0.301	0.181	0.302	0.181	0.302	0.189	0.307	0.185	0.306
	336	0.341	0.421	0.335	0.418	0.343	0.425	0.343	0.425	0.335	0.417	0.339	0.421
	720	0.879	0.701	1.014	0.765	0.881	0.704	0.881	0.704	0.890	0.707	0.895	0.709

Table 10: The ablation results of re-parameter mechanism.

W/ Reparameter							W/O Reparameter					
Metric	Accuracy	F1 Score	Accuracy	F1 Score	Accuracy	F1 Score	Accuracy	F1 Score	Accuracy	F1 Score	Accuracy	F1 Score
Setting	[7,7,7,7,7]		[7,7,7,13,13,13]		[7,7,13,13,19,19]		[7,7,7,7,7]		[7,7,7,13,13,13]		[7,7,13,13,19,19]	
CT	0.992	0.991	0.995	0.995	0.995	0.995	0.992	0.991	0.992	0.992	0.991	0.990
FM	0.640	0.632	0.643	0.641	0.680	0.677	0.623	0.619	0.637	0.635	0.630	0.625
JV	0.990	0.989	0.987	0.987	0.990	0.990	0.981	0.980	0.981	0.981	0.982	0.981
Setting	[19,19,19,19,19,19]		[19,19,19,29,29,29]		[19,19,29,29,37,37]		[19,19,19,19,19,19]		[19,19,19,29,29,29]		[19,19,29,29,37,37]	
CR	0.982	0.981	0.977	0.976	0.986	0.986	0.977	0.976	0.986	0.986	0.963	0.960
AWR	0.984	0.984	0.982	0.982	0.987	0.987	0.981	0.981	0.979	0.979	0.978	0.978
EC	0.347	0.267	0.338	0.273	0.338	0.249	0.321	0.286	0.321	0.296	0.295	0.274
PEMS	0.803	0.797	0.847	0.843	0.830	0.823	0.846	0.841	0.852	0.845	0.856	0.852
DDG	0.573	0.540	0.580	0.578	0.660	0.652	0.513	0.500	0.567	0.544	0.540	0.509
Setting	[37,37,37,37,37,37]		[37,37,37,43,43,43]		[37,37,43,43,53,53]		[37,37,37,37,37,37]		[37,37,37,43,43,43]		[37,37,43,43,53,53]	
EP	0.988	0.988	0.981	0.981	0.988	0.988	0.961	0.959	0.978	0.977	0.966	0.965
SRS	0.585	0.579	0.580	0.562	0.596	0.594	0.567	0.564	0.569	0.547	0.552	0.516

G Full Results

In this section, we supplement the full experimental results of two tasks and include relevant analysis figures.

G.1 Time Series Forecasting

Figure 5 illustrates the results of all methods on the time series forecasting task. The statistics in the figure represent the average performance of all methods across four different predicted length settings on each dataset.

G.2 Time Series Classification

Figure 6 illustrates the critical difference diagram of classification task as presented in [Demšar, 2006]. The complete experimental result, shown in the Table 11, is a supplement to the results of Table 2 in the main text. We also present the full experimental results of effectiveness over the hierarchical structure in Table 12, which is a supplement to Table 4 in the main text.

Figure 7: The visualization of forecasting case, generated by various models under the input-336-predict-336 setting, is presented. The black lines represent the ground truth, while the orange lines represent the predicted values.

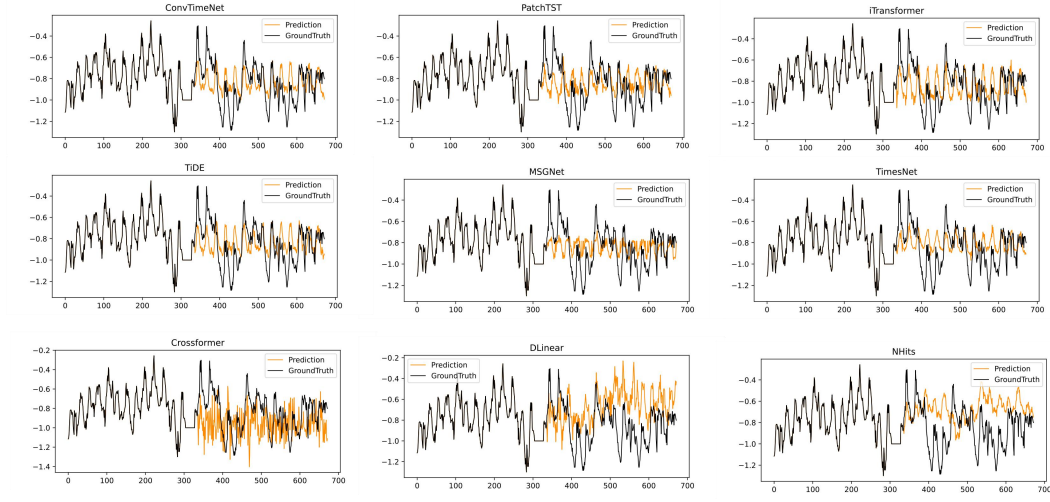


Figure 8: The visualization of deformable patch operation case. The black line represents the original sequence, the orange dotted line box indicates the uniform patch operation, while the blue dotted line box represents the deformable patch operation.

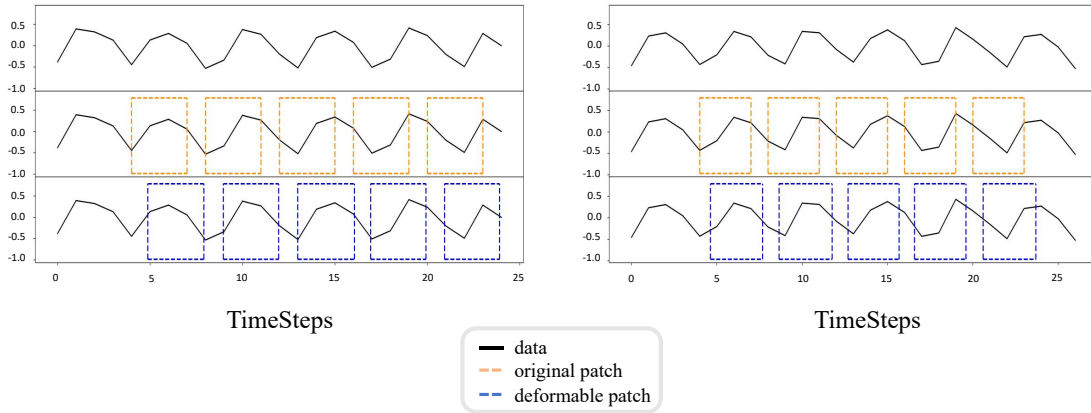


Table 11: Full results of time series classification task, in terms of Accuracy and F1 score. Noted that – indicates that the model cannot run due to the issue of being out of memory.

Metric	Dataset	ConvTimeNet	FormerTime	TimesNet	MiniRocket	TST	MLP	TCN	MCNN	MCDCNN
Accuracy	AWR	0.987	0.978	<u>0.980</u>	0.972	<u>0.980</u>	0.960	0.884	0.977	<u>0.980</u>
	CR	0.986	0.917	<u>0.889</u>	<u>0.981</u>	<u>0.898</u>	0.935	0.868	0.917	0.870
	CT	0.995	<u>0.992</u>	0.984	0.987	0.990	0.955	0.968	0.991	0.988
	EC	0.338	0.312	0.287	<u>0.327</u>	-	0.309	0.299	0.293	0.298
	EP	<u>0.988</u>	0.952	0.902	0.993	0.901	0.961	0.942	0.961	0.971
	FM	0.680	<u>0.650</u>	0.610	0.638	0.580	0.607	0.580	0.597	0.617
	JV	0.990	<u>0.986</u>	0.981	<u>0.987</u>	0.986	0.983	0.974	0.977	0.978
	PEMS	0.830	0.173	0.728	0.795	0.778	0.761	0.669	<u>0.804</u>	0.792
	SRS	0.596	0.572	0.542	0.564	0.541	0.546	0.507	<u>0.574</u>	0.565
	DDG	0.660	0.240	0.400	0.620	0.340	0.280	0.200	0.213	<u>0.624</u>
F1 Score	AWR	0.987	0.978	<u>0.980</u>	0.970	<u>0.980</u>	0.959	0.883	0.977	<u>0.980</u>
	CR	0.986	0.918	<u>0.886</u>	<u>0.980</u>	<u>0.890</u>	0.929	0.861	0.906	<u>0.863</u>
	CT	0.995	<u>0.991</u>	0.983	<u>0.986</u>	0.989	0.949	0.966	0.990	0.987
	EC	0.249	<u>0.261</u>	0.181	0.298	-	0.248	0.221	0.234	0.241
	EP	0.988	<u>0.950</u>	0.896	0.990	0.899	0.961	0.940	0.960	0.971
	FM	0.677	<u>0.628</u>	0.604	0.620	0.568	0.602	0.572	0.586	0.605
	JV	0.990	0.984	0.980	<u>0.988</u>	0.986	0.982	0.975	0.974	0.976
	PEMS	0.823	0.042	0.720	0.786	0.771	0.747	0.613	<u>0.799</u>	0.788
	SRS	0.594	<u>0.579</u>	0.507	<u>0.515</u>	0.487	0.516	0.371	0.573	0.565
	DDG	0.652	<u>0.113</u>	0.290	<u>0.622</u>	0.227	0.148	0.067	0.092	0.600

Table 12: Full results of studying the effectiveness of deep hierarchical architecture in terms of Accuracy and F1 score.

Metric	Hierarchy	One Stage			Two Stages			Three Stages	
Accuracy	Setting	[7,7,7,7,7,7]	[13,13,13,13,13,13]	[19,19,19,19,19,19]	[7,7,7,13,13,13]	[7,7,7,19,19,19]	[13,13,13,19,19,19]	[7,7,13,13,19,19]	
	CT	0.992	0.994	0.995	0.995	0.993	0.995	0.995	
	FM	0.640	0.680	0.653	0.643	0.660	0.630	0.680	
	JV	0.990	0.990	0.988	0.987	0.991	0.992	0.990	
	Setting	[19,19,19,19,19,19]	[29,29,29,29,29,29]	[37,37,37,37,37,37]	[19,19,19,29,29,29]	[19,19,19,37,37,37]	[29,29,29,37,37,..37]	[19,19,29,29,37,37]	
	CR	0.982	0.977	0.982	0.977	0.958	0.972	0.986	
	AWR	0.984	0.982	0.975	0.982	0.980	0.979	0.987	
	EC	0.347	0.345	0.342	0.338	0.340	0.337	0.338	
	PEMS	0.803	0.807	0.829	0.847	0.819	0.807	0.830	
	DDG	0.573	0.560	0.500	0.580	0.513	0.513	0.660	
	Setting	[37,37,37,37,37,37]	[43,43,43,43,43,43]	[53,53,53,53,53,53]	[37,37,37,43,43,43]	[37,37,37,53,53,53]	[43,43,43,53,53,53]	[37,37,43,43,53,53]	
	EP	0.988	0.983	0.981	0.981	0.978	0.976	0.988	
	SRS	0.585	0.570	0.589	0.580	0.582	0.589	0.596	
	F1 Score	Setting	[7,7,7,7,7,7]	[13,13,13,13,13,13]	[19,19,19,19,19,19]	[7,7,7,13,13,13]	[7,7,7,19,19,19]	[13,13,13,19,19,19]	[7,7,13,13,19,19]
		CT	0.991	0.994	0.995	0.995	0.993	0.994	0.995
		FM	0.632	0.676	0.651	0.641	0.657	0.629	0.677
		JV	0.989	0.990	0.988	0.987	0.993	0.991	0.990
Setting		[19,19,19,19,19,19]	[29,29,29,29,29,29]	[37,37,37,37,37,37]	[19,19,19,29,29,29]	[19,19,19,37,37,37]	[29,29,29,37,37,..37]	[19,19,29,29,37,37]	
CR		0.981	0.977	0.981	0.976	0.958	0.972	0.986	
AWR		0.984	0.982	0.974	0.982	0.980	0.979	0.987	
EC		0.267	0.304	0.298	0.273	0.267	0.265	0.249	
PEMS		0.797	0.798	0.819	0.843	0.812	0.801	0.823	
DDG		0.540	0.527	0.496	0.578	0.521	0.452	0.652	
Setting		[37,37,37,37,37,37]	[43,43,43,43,43,43]	[53,53,53,53,53,53]	[37,37,37,43,43,43]	[37,37,37,53,53,53]	[43,43,43,53,53,53]	[37,37,43,43,53,53]	
EP		0.988	0.983	0.981	0.981	0.979	0.975	0.988	
SRS		0.579	0.569	0.579	0.562	0.569	0.563	0.594	